Characterization of Large Amplitude Motions and Hydrogen Bonding Interactions in the Thiophene–Water Complex by Rotational Spectroscopy

Weslley G. D. P. Silva and Jennifer van Wijngaarden*

Department of Chemistry, University of Manitoba, Winnipeg, Manitoba, R3T 2N2, Canada

*Corresponding author

Email: vanwijng@cc.umanitoba.ca

Phone: (204)474-8379

Fax: (204)474-7608

Abstract

The rotational fingerprint of the thiophene–water complex was investigated for the first time using Fourier transform microwave spectroscopy (7–20 GHz) aided by quantum mechanical calculations. Transitions for a single species were observed and the rotational constants for the parent and ^{18}O isotopomers are consistent with a geometry that is highly averaged over a barrierless large amplitude motion of water that interconverts two equivalent forms corresponding to the global minimum (B2PLYP-D3(BJ)/def2-TZVP). In this effective geometry, the water lies above the thiophene ring close to its σ_v plane of symmetry. The observed transitions are split by a second water-centered tunneling motion that exchanges its two protons by internal rotation about its C_2 axis with a calculated barrier of ~2.7 kJ mol^{-1} (B2PLYP-D3(BJ)/def2-TZVP). Based on quantum theory of atoms in molecules, non-covalent interaction and symmetry-adapted perturbation theory analyses, the observed geometry enables two intermolecular interactions (O–H$\cdots\pi$ and O–H$\cdots$S) whose electrostatic and dispersive contributions favour formation of the thiophene-water complex.

Introduction

Non-covalent interactions involving aromatic rings play a key role in many chemical and biological processes such as molecular recognition, aggregation and protein folding.[1,2] Despite their importance, accurate experimental and computational descriptions of the molecular level forces involved in solvation of an aromatic molecule remain challenging even for small prototypical systems such as 1:1 solvent–solute molecular aggregates.[3–5] When a solvent molecule approaches an aromatic ring, interactions may be formed with the π-electron clouds of the ring, either at its center or on a C=C bond, or with the aromatic hydrogens in which the solvent may serve as a proton donor and/or acceptor.[6] The scenario is more complicated for aromatic heterocycles as additional contacts may be established with the heteroatom.[3–5,7,8] The presence of multiple potential binding sites with interaction energies that are often sensitive to the computational levels chosen affirm the importance of experimental studies of isolated solvent-solute complexes.

Coupled with the complexity described above, rotational spectroscopic studies of the monohydrated complexes of pyrrole (pyrrole–w)[4,9], pyridine (pyridine–w)[5] and thiazole (thiazole–w)[8] revealed that due to a shallow potential energy surface around the global minimum geometry, the ground state structures of these complexes, stabilized by N–H···O (pyrrole–w) and N···H–O (pyridine–w and thiazole–w) hydrogen bonds (HB) in which the oxygen atom of water lies in the same plane as the heterocyclic structure, are highly influenced by large amplitude motions. These motions (not typically captured by routine computational methods) are associated with the internal dynamics of water and may lead to tunneling splittings in the rotational spectrum depending on the barrier height. Although

the water complexes of the oxygen and sulfur counterparts of pyrrole, namely furan and thiophene, have not been investigated by rotational spectroscopy, their vibrational spectra were reported by Ar matrix FTIR (Fourier transform infrared) spectroscopy.[10] While for furan–w the IR spectrum was consistent with a single geometry with the oxygen of water in the plane of the ring and stabilized by a O–H···O HB in agreement with computational results,[7] for thiophene–w, the dominant species in the matrix is governed by a weak CH···O interaction with all heavy atoms in one plane. This was rather unexpected as the lowest energy conformer is predicted to have the water molecule above the plane of the thiophene ring and to be stabilized by a O–H···π interaction.[10] The vibrational spectrum of thiophene–w thus raises the question of whether the preferred binding site of water in this complex is in fact ruled by a C–H···O interaction or if the observed results were affected by matrix effects. In any case, previous investigations have shown that water preferentially binds to the more electronegative heteroatoms in pyrrole, pyridine, thiazole and furan (with the oxygen of water lying in the same plane as the ring) whereas interactions with thiophene are intrinsically different in nature. This is likely due to the less electronegative sulfur atom.

Herein, we describe the first investigation of the thiophene–w complex using high resolution rotational spectroscopy to resolve the discrepancy between experiment (matrix IR) and theory in terms of the most stable geometry of the dimer. Rotational spectroscopy is the ideal tool for this as the patterns of transitions are governed by the moments of inertia providing confirmation of the underlying geometry. Additionally, the supersonic jet is a collision-free environment where species are studied in isolation of solvent and matrix effects. Our combined quantum chemical and spectroscopic study establishes that the

ground state structure of thiophene–w is highly averaged over a barrierless large amplitude motion that interconverts two equivalent forms of the complex corresponding to the global minimum. The interactions governing the formation of the complex were investigated using quantum theory of atoms in molecules (QTAIM)[11] and non-covalent interaction (NCI)[12] analyses. The nature of the intermolecular interactions forming the thiophene–w complex were studied using symmetry-adapted perturbation theory (SAPT)[13] calculations and are compared with theoretical results derived here for the related species pyrrole–w, furan–w and benzene–w. The analyses show that the observed complex is stabilized by O–H···π and O–H···S HB while SAPT calculations show that thiophene behaves more like a benzene molecule when binding to water than other heterocycles.

Experimental Methods

The rotational fingerprints of the thiophene–w complex were investigated from 7–20 GHz using a broadband chirped-pulse (cp) and a cavity-based Balle-Flygare (BF) type Fourier transform microwave (FTMW) spectrometer. Both instruments have been described in detail previously.[14,15] To produce the complex, a gas mixture of ~1% thiophene (99%, bp: 357K, Sigma-Aldrich Canada) seeded in neon was prepared at room temperature and subsequently bubbled through a reservoir containing water (or water enriched with ^{18}O for isotopic measurements). The resulting gas mixture (thiophene + water) was then delivered inside the high vacuum chambers (P ~ 10^{-7} kPa) of the instruments using a pulsed nozzle (1 mm orifice) which creates a supersonic jet expansion. In the jet, the molecules are probed in a collision-free environment where the rotational temperature is

cooled to a few Kelvin. Initially, a broadband survey spectrum was collected with the cp-FTMW instrument from 8–18 GHz in segments of 2 GHz from which the most intense rotational transitions of the parent and ^{18}O species of the thiophene–w complex were identified. Final frequency measurements were performed using the BF-FTMW spectrometer from 7–20 GHz which features higher resolution and sensitivity. In a typical BF-FTMW experiment, the recorded transitions have widths of ~7 kHz (FWHM) while the uncertainty in line positions is ±2 kHz. The transitions are split into two Doppler components due to the collinear arrangement of the molecular beam and the resonator axis.

Computational Methods

The possible geometries of the thiophene–w complex were identified by performing a conformational search using the conformer-rotamer ensemble sampling tool (CREST)[16] as implemented in the extended tight binding (xTB) program.[17] The search found 28 plausible structures for the complex which were fully optimized at the double-hybrid B2PLYP[18]-D3(BJ)[19,20]/def2-TZVP[21] level of theory. For the optimization calculations, we used a tight convergence criteria given the characteristic shallow potential energy surface of related water complexes and included the Boys and Bernardi's counterpoise[22] method to account for the basis set superposition error (BSSE). Harmonic frequency calculations were also carried out at the same level of theory to verify the nature of the stationary points and to obtain relative energies with zero-point correction (ZPE) and quartic centrifugal distortion constants. The optimization and frequency calculations confirmed the presence of only four unique conformers (out of the 28 initial geometries

from CREST) for thiophene–w at the B2PLYP-D3(BJ)/def2-TZVP level. To obtain energy barriers associated with the interconversion between conformers, transition state structures were optimized at the B2PLYP-D3(BJ)/def2-TZVP level and were confirmed to be true by the presence of a single imaginary frequency. All optimization and frequency calculations were carried out using the Gaussian 16 program.[23]

To visualize the intermolecular interactions occurring in thiophene–w, we performed QTAIM[11] and NCI[12] analyses using the AIMALL[24] and NCIPLOT[25] programs, respectively. The nature behind the formation of the thiophene–w dimer was further investigated by decomposing the complex interaction energy into four physically meaningful components (electrostatic, dispersion, induction and exchange) using a SAPT analysis.[13] We also carried out SAPT calculations for related complexes such as furan–w, pyrrole–w and benzene–w and compare the results with those obtained for thiophene–w. All SAPT calculations were performed at the SAPT2+(3)δMP2[26]/def2-TZVP level using the Psi4 code.[27]

Results

The conformational search using CREST followed by higher level quantum chemical calculations suggest that water can interact with thiophene to form four stable conformers (I, II, III and IV, Figure 1) numbered in order of increasing energy. The Cartesian coordinates for their equilibrium structures at the B2PLYP-D3(BJ)/def2-TZVP level are given in Tables S1-S4 of the supporting information (SI) file. The calculated zero-point corrected relative energies, rotational constants and electric dipole moment components of each conformer are provided in Table 1. Although these four conformers

have been reported[10] theoretically, we decided to extend the computational work on the thiophene–w complex to include B2PLYP-D3(BJ)/def2-TZVP calculations. This level of theory is known[4,8,28] to provide accurate estimates for the rotational parameters of water complexes facilitating the assignment of the different species in the rotational spectrum.

Based on the quantum mechanical calculations from Table 1, conformer I is predicted to be the global minimum geometry for the complex and appears to be stabilized by O–H···π interactions in which one hydrogen of water binds to the π-orbital of a C=C bond while the other hydrogen atom is directed above the middle of the ring (Figure 1). This is contrary to the most stable conformer reported for the monohydrates of furan (O···H–O),[7] pyrrole (N–H···O)[4], thiazole (N···H–O)[8] and pyridine (N···H–O)[5] where the center of mass of water lies in the plane of the ring such that water binds to the most electronegative heteroatom or with the hydrogen attached to it in the case of pyrrole. The structure reported to be the most abundant based on the Ar matrix IR spectrum,[10] forming a C–H···O HB (conformer II in this work), is predicted to be at least 2.4 kJ mol^{-1} (Table 1) less stable than conformer I at the B2PLYP-D3(BJ)/def2-TZVP level.

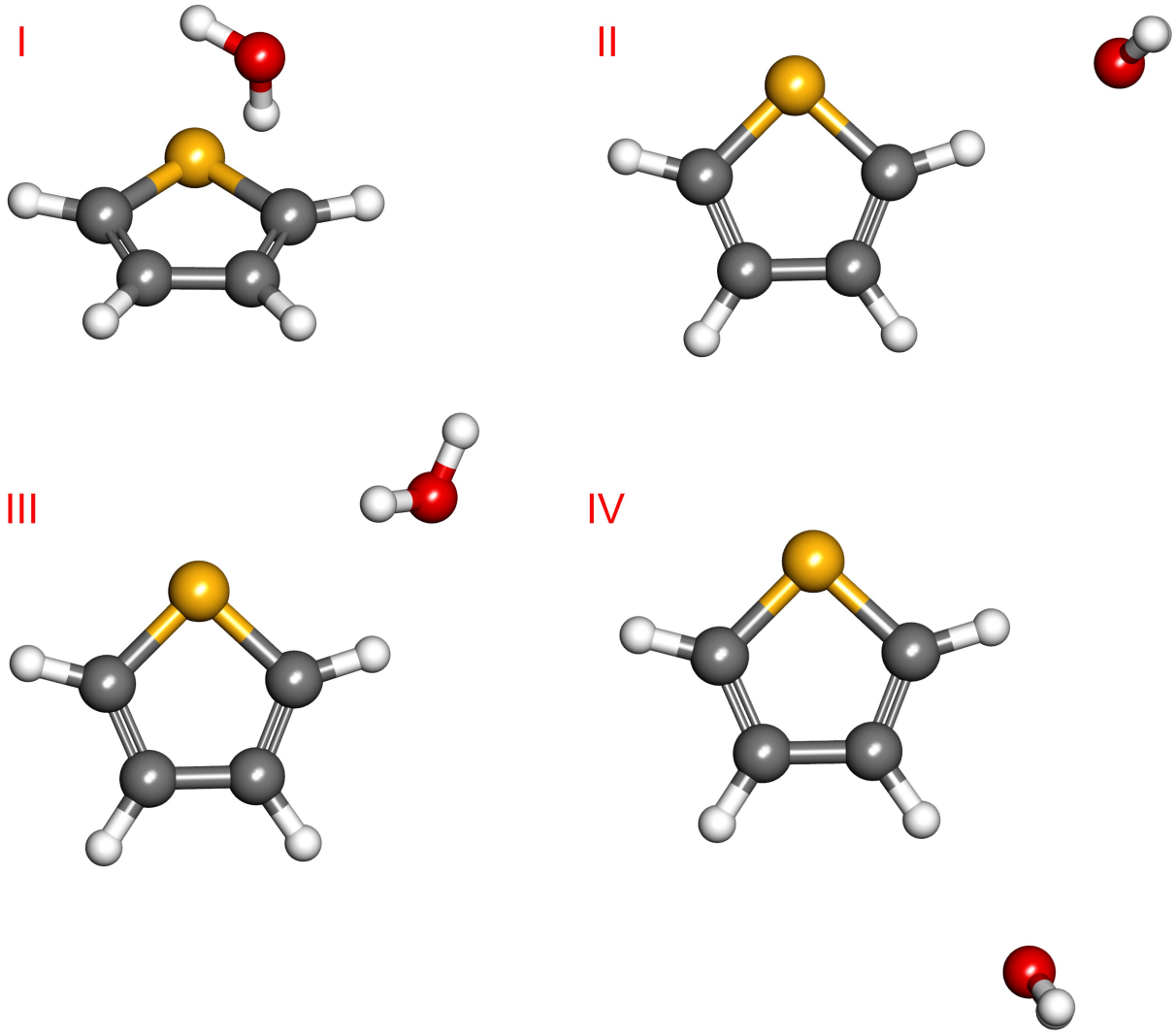

Figure 1. Four conformers of the thiophene–w complex obtained at the B2PLYP-D3(BJ)/def2-TZVP level of theory.

Table 1. Calculated relative energies with zero-point correction (ΔE_{ZPE}), rotational constants (*A*, *B*, *C*) and electric dipole moment components for the conformers of the thiophene–w complex obtained at the B2PLYP-D3(BJ)/def2-TZVP level of theory.

Conformer	ΔE_{ZPE} (kJ mol^{-1})	*A*/*B*/*C* (MHz)	$\mu_a/\mu_b/\mu_c$ (Debye)
I	0.0	3461/1983/1788	2.2/0.5/0.7
II	2.4	5550/1325/1075	2.4/0.3/0.0
III	2.5	5845/1587/1287	0.8/0.9/1.1
IV	4.4	7030/1092/949	3.0/0.0/0.0

As the rotational signature of the thiophene–w complex has not been previously reported, the calculated parameters from Table 1 were used to guide the spectroscopic assignment. In the rotational spectrum, we observed transitions belonging to the thiophene monomer and new sets of lines which were assigned to conformer I of thiophene–w. The assigned lines were *a*-type R-branch transitions, consistent with the large $|\mu_a|$= 2.2 D for conformer I and showed a tunneling splitting which was readily recognized in the cp-FTMW spectrum. The assignments were confirmed by measuring transitions for the singly substituted ^{18}O species (obtained from experiments using $H_2{}^{18}O$) which were also split into tunneling doublets. For both parent and ^{18}O species, the tunneling components presented an intensity ratio of ~3:1 based on the cavity BF-FTMW measurements. The two tunnelling states for each isotopomer were fitted independently with Pickett's SPFIT program[29] using a Watson's S-reduced Hamiltonian (I^r representation)[30] to yield the spectroscopic parameters shown in Table 2. The complete line lists containing the transition frequencies and fit residuals are given in Tables S5–S6. The transitions for the two tunneling states were labeled as 'lower' and 'upper' in Table 2 which refer to the sets of lines observed at lower and higher frequency, respectively. Despite the sizeable $|\mu_b|$= 0.5 D and $|\mu_c|$= 0.7 D dipole components predicted for conformer I and a careful search, neither *b*- nor *c*-type transitions could be observed in the spectrum. Transitions consistent with other conformers of thiophene–w were not observed despite the fact that the a-dipole of conformer II is predicted to be greater than that of conformer I.

Table 2. Spectroscopic parameters obtained for the observed species of the thiophene-w complex.

	Parent			^{18}O		
Parameter	Lower	Upper	Average	Lower	Upper	Average
A/MHz[a]	3300.1290(71)	3340.8600(76)	3320.4945	3294.40(11)	3334.33(24)	3314.365
B/MHz	2089.06830(34)	2093.94782(35)	2091.50806	1961.2425(25)	1965.9168(27)	1963.57965
C/MHz	1879.73050(24)	1885.01782(25)	1882.37416	1773.7528(25)	1778.5700(35)	1776.1614
D_J/kHz[b]	6.5214(48)	6.0429(52)	12.5643	5.73(12)	5.19(16)	5.46
D_{JK}/kHz	39.537(47)	34.503(50)	37.020	[39.537][e]	[34.503]	37.020
d_1/kHz	-1.2704(44)	-1.1675(44)	1.21895	[-1.2704]	[-1.1675]	1.21895
d_2/kHz	0.2545(36)	0.1234(54)	0.18895	[0.2545]	[0.1234]	0.18895
N[c]	29			13		
σ/kHz[d]	0.7			4.8		

[a]Rotational constants (*A*, *B* and *C*), [b]quartic distortion constants (D_J, D_{JK}, d_1, d_2), [c]number of fitted transitions (*N*), [d]standard deviation of the fit (σ); [e]Values in brackets [ ] were fixed to the value derived for the parent species. A complete list containing the calculated constants obtained at the B2PLYP-D3(BJ)/def2-TZVP level is provided in Table S7.

Discussion

Based on comparison of the experimentally-derived rotational constants with the quantum chemical predictions from Table 1, it is evident that the measured spectrum of thiophene–w is closest to that expected for conformer I, the global minimum geometry. This establishes that the O–H···π HB is the dominant interaction that favours complex formation. Our results, based on the rotational spectrum of the isolated dimer, differ from those derived from IR experiments in which the C–H···O bound conformer II was purported to be the major species, however, this may have been influenced by matrix effects.[10] Although the experimental rotational constants (Table 2) for conformer I are consistent with the calculated values (Table 1), the discrepancies are larger than one might expect as are the differences in the centrifugal distortion constants (Tables 2, S7). From the absence of *b*- and *c*-type transitions and the observation of a tunneling splitting in the spectrum, it is clear that internal motions associated with the water molecule must be investigated to understand the spectrum of thiophene–w. In previous studies of the related pyrrole–w,[4,9] thiazole–w[8] and pyridine–w[5] complexes, for example, no *c*-type transitions were detected in the rotational spectrum despite sizeable $|\mu_c|$ due to internal dynamics of water which average the dipole along the *c*-axis to zero.

Based on the geometry of conformer I as shown in Figure 2, there is an equivalent form in which the O–H···π interaction is established on the opposite side of thiophene's σ_v plane. In Figure 2, we investigate two possible pathways (Path 1 and Path 2) for interconversion between Ia and Ib and their corresponding transition states whose natures are confirmed by the observation of a single imaginary frequency at the B2PLYP-D3(BJ)/def2-TZVP. The calculated energy barriers for Path 1 and Path 2 are very low; on

the order of 0.4 kJ mol^{-1} and 0.8 kJ mol^{-1} (B2PLYP-D3(BJ)/def2-TZVP). When ZPE corrections are taken into consideration, the interconversion between Ia and Ib is essentially barrierless as the barriers are lowered to -0.2 kJ mol^{-1} for Path 1 and 0.4 kJ mol^{-1} for Path 2. This implies that the ground state structure is an effective one lying somewhere between that of Ia and Ib. The observation of averaged ground state structures as a consequence of large amplitude motions have been previously reported for monohydrated complexes of small heterocycles[4,8] and flexible molecules such as 2-fluoroethanol.[31]

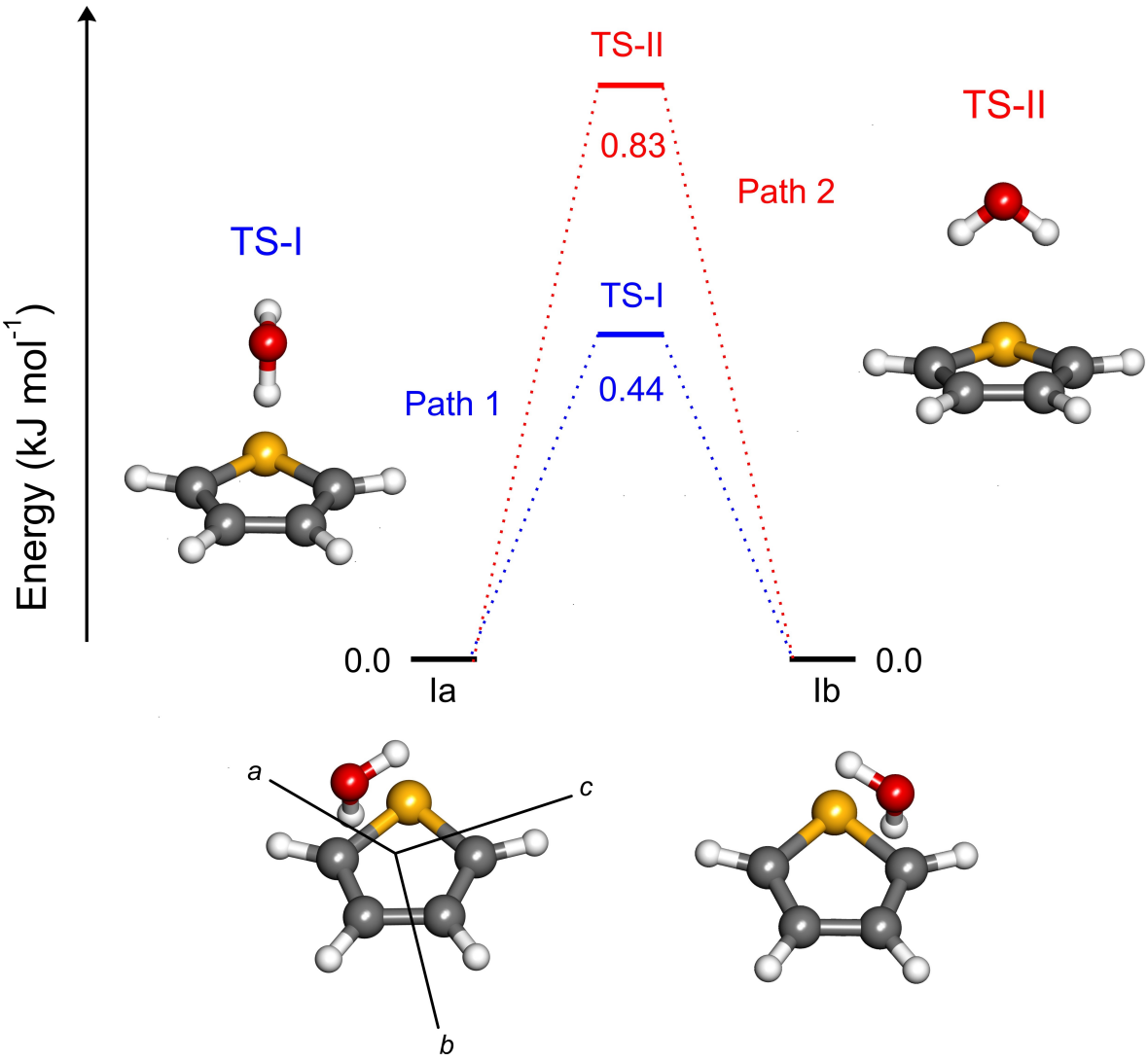

Figure 2. Possible pathways (Path 1 and Path 2) and transitions states (TS-I and TS-II) for the interconversion between the two equivalent forms of conformer I (Ia and Ib) obtained at the B2PLYP-D3(BJ)/def2-TZVP level.

To better characterize the ground state geometry, we first used the experimental rotational constants of the singly substituted ^{18}O isotopomer to derive Kraitchman's[32] substituted r_s atomic coordinates (Table 3) for the oxygen of water using the KRA program.[29] It is important to note that the obtained |c| coordinate was set to zero since it yielded an imaginary value in the analysis suggesting that the oxygen atom is close to the

ab-plane of the complex. In Figure 3, we compare the position of water in the equilibrium geometry of conformer I and in the two transitions states (TS-I and TS-II); the atomic coordinates for these geometries are also given in Table 3. From the *c*-coordinates in particular, it is evident that the ground state geometry is closer to that of TS-I and TS-II (but slightly closer to that of TS-I) than to the equilibrium geometry of conformer I. To describe the geometry of thiophene–w in terms of the principal axis system of the thiophene monomer,[33] a Kraitchman analysis was also performed treating the water molecule (mass 18.01056 amu) as a substitution site of the thiophene monomer. This provided substitution coordinates {*a*, *b*, *c*} with absolute values of 0.523(3) Å, 0.267(6) Å and 3.3801(5) Å which places the center of mass of water slightly out of the *ac*-plane (σ_v) of thiophene (0.267(6) Å) which would be analogous to the *c*-coordinate in the TS of the thiophene-w complex (Figure 3 top). While this value may seem consistent with the magnitude of the *c*-coordinate of conformer I in its equilibrium form in Table 3, it is important to note that the axis system is shifted and rotated slightly in conformer I by comparison as shown in Figure 2. A more realistic picture of the position of water relative to the σ_v plane of thiophene in conformer I is seen in Figure 3 in the bottom left corner. As the oxygen atom (and its center of mass) is above the C=C bond, we can estimate that the distance to the σ_v plane of thiophene is around half the C–C bond distance (~1.4 Å). This result from treating water as a point is consistent with the other Kraitchman results in Table 3 that the ground state geometry is closer to that of a TS geometry than the equilibrium geometry.

Table 3. Kraitchman's coordinates (in Ångstroms) with associated Costain errors obtained for the oxygen atom of water from the observed tunnelling states (Lower, Upper) and quantum chemical calculations (I, TS-I, TS-II). Refer to Figures 2 and 3 for the axis systems from the equilibrium and transition state structures.

	$\|a\|$	$\|b\|$	$\|c\|$
Lower	2.8293(6)	0.411(4)	0[a]
Upper	2.8245(7)	0.432(5)	0[a]
I	2.91	0.45	0.28
TS-I	2.87	0.51	0.00
TS-II	2.80	0.56	0.00

[a]Set to zero due to the presence of an imaginary value.

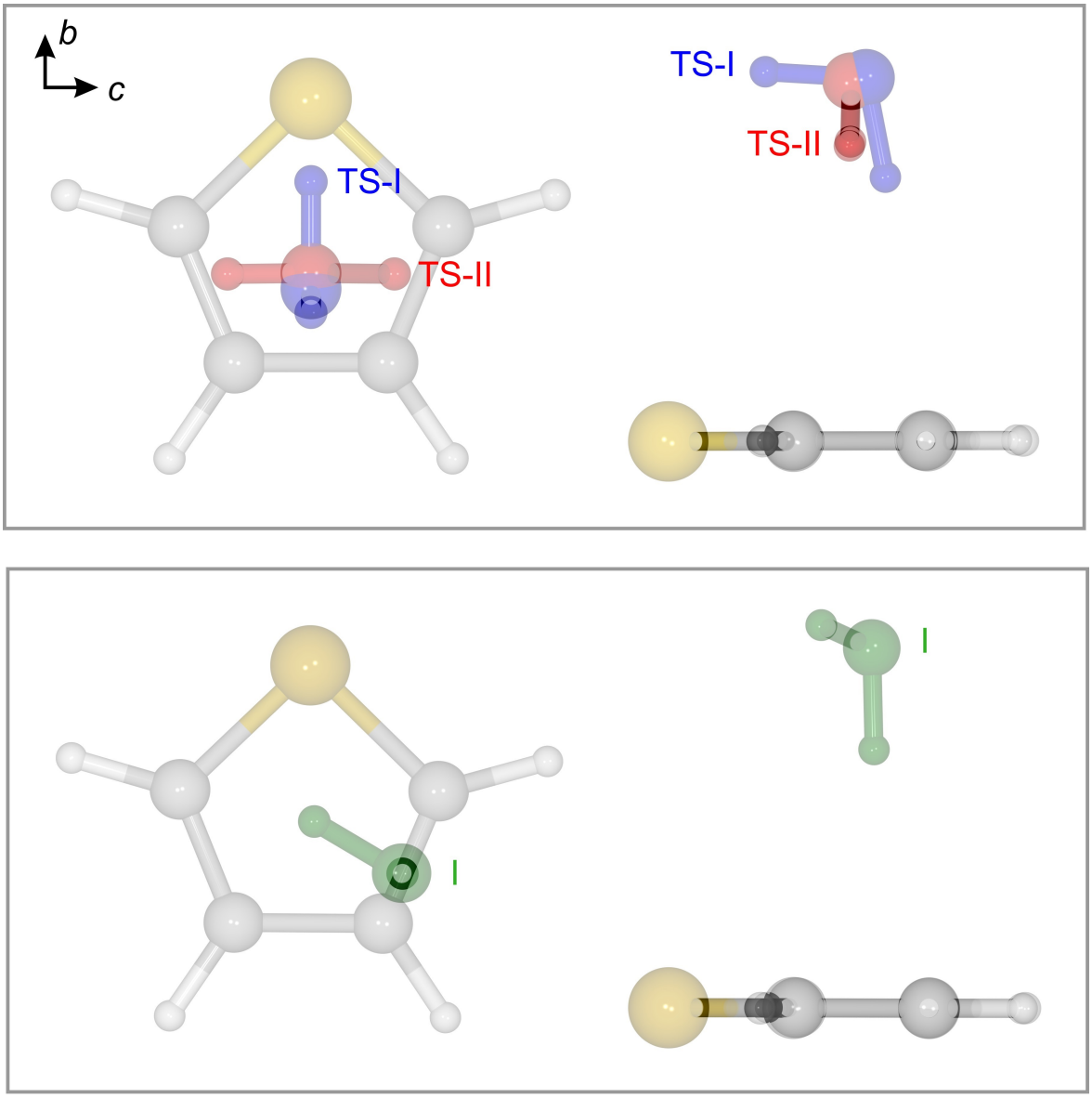

Figure 3. Comparison of the position of water in the equilibrium geometry of conformer I (green), TS-I (blue) and TS-II (red). Note that the axis system in the equilibrium geometry (bottom) is that given in Figure 2.

Additional information about the location of the water molecule within the complex can be derived from the planar moments of inertia obtained from the rotational constants. The P_{cc} values for the parent (62.26 amu Å^2 and 63.10 amu Å^2 for the upper and lower tunneling states, respectively) and ^{18}O species (62.25 amu Å^2 and 63.10 amu Å^2) of thiophene–w, are very similar to the P_{bb} value reported for the thiophene monomer (62.87 amu Å^2).[34] This suggests that the water molecule lies largely in thiophene's σ_v plane of symmetry. Similar results have been observed for the thiophene–HBr and thiophene–HCl complexes in which the HBr and HCl subunits are located on the σ_v plane of the thiophene ring.[34] By comparing the experimental P_{cc} values of thiophene–w with those predicted computationally for conformer I (59.12 amu Å^2), TS-I (62.57 amu Å^2) and TS-II (63.65 amu Å^2), the P_{cc} values of TS-I and TS-II (in particular TS-I) are closer to the experimentally derived values which lends further support to the position of the oxygen atom in the highly averaged ground state structure.

The observation of a structure with the oxygen centered above the thiophene ring as in TS-I and TS-II is also consistent with the lack of *c*-type transitions in the spectrum as a motion via these transition states would average the dipole along the *c*-axis to zero as reported for pyrrole–w,[4,9] thiazole–w[8] and pyridine–w.[5] The absence of *b*-type transitions indicates that the ground state structure is more similar to TS-I as the predicted μ_b for this geometry is -0.1 D (B2PLYP-D3(BJ)/def2-TZVP) (compared with 0.5 D in conformer I and 1.2 D in TS-II). While the μ_b dipole component does not average to zero if the thiophene–w complex passes through TS-I, its magnitude would be a very small relative to that of the μ_a dipole of 2.2 D which is consistent with our inability to observe *b*-type transitions. Collectively, the above observations from Kraitchman's analysis, planar

moments and selection rules, suggest that the water subunit undergoes a large amplitude motion within the thiophene–w complex via TS-I (Figure 2).

The rotational transitions of thiophene-w also displayed a tunneling splitting and as the large amplitude motion between Ia and Ib is essentially barrierless, this is likely associated with exchange of the two hydrogens of water via inertial rotation along its C_2 axis. We estimated the barrier of this motion in the thiophene–w complex to be of about 2.7 kJ mol^{-1} (B2PLYP-D3(BJ)/def2-TZVP) based on the geometry of TS-I. An analogous internal rotation of water led to tunneling splittings in the pyrrole–w[4,9] and pyridine–w[5] dimers.

With novel insights regarding the effective ground state structure of the thiophene–w complex (compared with those of other heterocycles), we analyzed the interactions responsible for the formation of the dimer using QTAIM,[11] NCI,[12] and SAPT[13] calculations. The calculations were performed for the optimized TS-I geometry since it is a reasonable model of the observed averaged ground state structure. In the QTAIM molecular graph of thiophene–w (Figure 4), a bond path (black dotted line) and a bond critical point (BCP, green dot) are observed between one hydrogen of water which acts as a HB donor and the C=C bond suggesting that a primary O–H···π interaction is responsible for the formation of the complex. Based on the electron potential energy (V) at the BCP, an interaction strength of ~5.1 kJ mol^{-1} (E= 0.5V)[35] is obtained for the O–H···π HB which is approximately 4.6 times weaker than the O–H···N HB reported for thiazole–w[8] for comparison. Although the observed geometry of thiophene–w seems to favour an additional S···H–O interaction, the QTAIM analysis did not detect it. This means that this interaction is either absent in thiophene–w or not strong enough to be captured by the

QTAIM method. Thus, we also performed NCI calculations which is a more suitable approach for describing weaker, long-range interactions. The NCI isosurfaces (Figure 4), obtained from the electron density and its derivatives, confirm the primary O–H···π HB but also show the existence of the secondary O–H···S contact in the complex in which water also acts as a HB donor. Both interactions are visualized by the blue-green isosurfaces in the interacting regions.

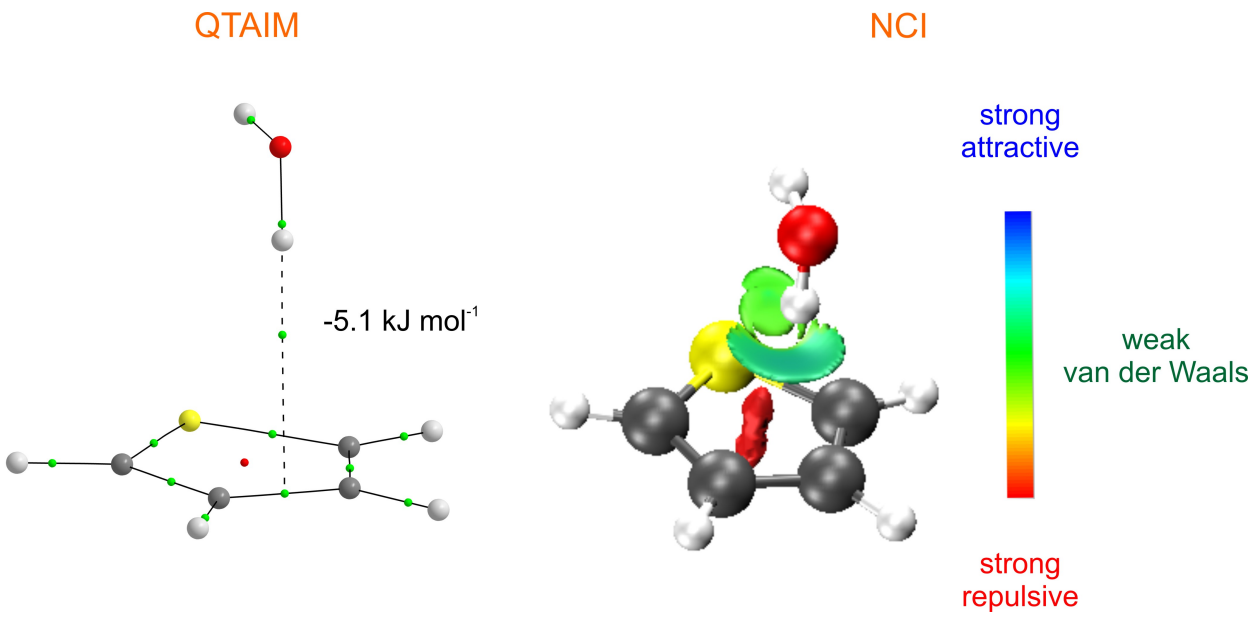

Figure 4. QTAIM molecular graph (left) and NCI isosurface (right, s=0.5 and colour scale BGR: 0.02 < ρ < +0.02) for the observed conformer of the thiophene–w complex.

While the QTAIM and NCI analyses provide descriptions of each intermolecular interaction, SAPT analysis gives more quantitative knowledge of the nature behind the formation of the complex. We compare the SAPT results of thiophene–w with those for pyrrole–w, furan–w and benzene–w in Table 3. The total SAPT energies indicate that pyrrole and furan form the most stable complexes with water due to larger contributions

from the electrostatic term. The preferred stability of these two complexes is consistent with the stronger N–H···O and O–H···O HBs they form with water in contrast to the weaker O–H···S and/or O–H···π HBs in thiophene–w and benzene–w. Although all complexes have the electrostatic energy as the most stabilizing term, representing at least ~48% of the total stabilization energy (electrostatic + repulsion + induction), a noticeable increase in the contributions from dispersion is observed from pyrrole–w (15.4%) < furan–w (22%) < thiophene–w (36.8%) ~ benzene–w (38.0%). In the monohydrates of thiophene and benzene, the electrostatic and dispersive contributions are much more balanced which supports the idea that the O–H···π HBs are weaker, longer-range interactions and more dispersive in nature. Overall, from the SAPT results in Table 3, the nature of the interactions binding thiophene to water are more similar to those of benzene–w than for those of heterocycles such as furan and pyrrole. The preference of water to interact primarily with the π-system in thiophene rather than to the heteroatom as in furan,[7] pyrrole[4,9] and thiazole[8] is explained by key differences in the electron density distribution in the heterocycles. While in furan and pyrrole the negative charges are concentrated around O and N due to their high electronegativity, in thiophene, the negative charge from the heteroatom is more dispersed into the ring making the π-systems the preferred binding site for the water molecule.[10,34]

Table 3. Symmetry-adapted perturbation theory results for thiophene–w, benzene–w, furan–w and pyrrole–w obtained at the SAPT2+(3)δMP2/def2-TZVP level of theory. The values in brackets ( ) represent the contribution of that term (in percentage) to the total stabilizing energy (electrostatic + induction + dispersion).

Complex	Total	Electrostatic	Induction	Dispersion	Exchange
Thiophene–w	-10.8	-11.6 (48.6%)	-3.5 (14.6%)	-8.8 (36.8%)	13.1
Benzene–w	-11.6	-13.5 (48.4%)	-3.8 (13.6%)	-10.6 (38.0%)	16.3
Furan–w	-12.1	-20.6 (59.6%)	-6.4 (18.4%)	-7.6 (22.0%)	22.5
Pyrrole–w	-22.4	-34.7 (65.9%)	-9.9 (18.7%)	-8.1 (15.4%)	30.3

Conclusions

Combining rotational spectroscopy and quantum mechanical calculations, the geometry of the thiophene–w complex was established for the first time in isolation of solvent and matrix effects. The observed spectrum is consistent with a geometry that is highly averaged over a barrierless large amplitude motion which interconverts the two equivalent forms of conformer I corresponding to the predicted global minimum at the B2PLYP-D3(BJ)/def2-TZVP level of theory. In this effective geometry, the water molecule lies above the thiophene ring close to its σ_v plane of symmetry and forms the complex via O–H···π and S···H–O HBs as supported by the experimentally-derived planar moments, substitution coordinates for the water oxygen (from ^{18}O measurements), QTAIM and NCI analyses. In addition to the above large amplitude motion, the transitions for the thiophene–w complex showed a tunneling splitting that is attributed to a water centered internal rotation about its C_2 axis which exchanges the protons of water with a calculated barrier of ~2.7 kJ mol^{-1} (B2PLYP-D3(BJ)/def2-TZVP). Based on SAPT results, we show

that a balance of electrostatic and dispersive forces contributes to the stabilization of the thiophene–w complex while for pyrrole–w and furan–w, the electrostatic term is dominant. This work on the thiophene–w dimer serves as a guide for future investigations on larger molecular complexes of thiophene with larger solvent shells.

Supporting Information

Appendix 1: Cartesian coordinates for the conformers of thiophene–w

Appendix 2: Assigned transitions and residuals for the observed conformer of thiophene–w

Appendix 3: Full set of calculated spectroscopic parameters for conformer I of thiophene–w

Acknowledgements

We acknowledge the Natural Sciences and Engineering Research Council of Canada (NSERC) for funding this research through the Discovery Grant program and the University of Manitoba for its computational research facility, GREX. W.G.D.P.S is also grateful for a University of Manitoba Fellowship (UMGF) provided by the Faculty of Graduate Studies.

References

(1) Nishio, M.; Umezawa, Y.; Fantini, J.; Weiss, M. S.; Chakrabarti, P. CH-π Hydrogen Bonds in Biological Macromolecules. *Phys. Chem. Chem. Phys.* **2014**, *16* (25), 12648–12683.

(2) Brandl, M.; Weiss, M. S.; Jabs, A.; Sühnel, J.; Hilgenfeld, R. C-H···π-Interactions

in Proteins. *J. Mol. Biol.* **2001**, *307* (1), 357–377.

(3) Gottschalk, H. C.; Poblotzki, A.; Fatima, M.; Obenchain, D. A.; Pérez, C.; Antony, J.; Auer, A. A.; Baptista, L.; Benoit, D. M.; Bistoni, G.; et al. The First Microsolvation Step for Furans: New Experiments and Benchmarking Strategies. *J. Chem. Phys.* **2020**, *152* (16), 164303.

(4) Wu, B.; Xie, F.; Xu, Y. The Pyrrole-Water Complex: Multidimensional Large Amplitude Dynamics and Rotational Spectra of Its ^{13}C Isotopologues. *J. Mol. Spectrosc.* **2020**, *374*, 111381.

(5) Mackenzie, R. B.; Dewberry, C. T.; Cornelius, R. D.; Smith, C. J.; Leopold, K. R. Multidimensional Large Amplitude Dynamics in the Pyridine-Water Complex. *J. Phys. Chem. A* **2017**, *121* (4), 855–860.

(6) Li, S.; Cooper, V. R.; Thonhauser, T.; Puzder, A.; Langreth, D. C. A Density Functional Theory Study of the Benzene−Water Complex. *J. Phys. Chem. A* **2008**, *112* (38), 9031–9036.

(7) Lockwood, S. P.; Fuller, T. G.; Newby, J. J. Structure and Spectroscopy of Furan:H_2O Complexes. *J. Phys. Chem. A* **2018**, *122* (36), 7160–7170.

(8) Li, W.; Chen, J.; Xu, Y.; Lu, T.; Gou, Q.; Feng, G. Unveiling the Structural and Energetic Properties of Thiazole-Water Complex by Microwave Spectroscopy and Theoretical Calculations. *Spectrochim. Acta - Part A Mol. Biomol. Spectrosc.* **2020**, *242*, 118720.

(9) Tubergen, M. J.; Andrews, A. M.; Kuczkowski, R. L. Microwave Spectrum and Structure of a Hydrogen-Bonded Pyrrole-Water Complex. *J. Phys. Chem.* **1993**, *97* (29), 7451–7457.

(10) Wasserman, J. G.; Murphy, K. J.; Newby, J. J. Evidence of C–H···O Interactions in the Thiophene:Water Complex. *J. Phys. Chem. A* **2019**, *123* (48), 10406–10417.

(11) Bader, R. F. W. Atoms in Molecules. *Acc. Chem. Res.* **1985**, *18* (1), 9–15.

(12) Johnson, E. R.; Keinan, S.; Mori-Sánchez, P.; Contreras-García, J.; Cohen, A. J.; Yang, W. Revealing Noncovalent Interactions. *J. Am. Chem. Soc.* **2010**, *132* (18), 6498–6506.

(13) Jeziorski, B.; Moszynski, R.; Szalewicz, K. Perturbation Theory Approach to Intermolecular Potential Energy Surfaces of van Der Waals Complexes. *Chem. Rev.* **1994**, *94* (7), 1887–1930.

(14) Evangelisti, L.; Sedo, G.; van Wijngaarden, J. Rotational Spectrum of 1,1,1-Trifluoro-2-Butanone Using Chirped-Pulse Fourier Transform Microwave Spectroscopy. *J. Phys. Chem. A* **2011**, *115* (5).

(15) Sedo, G.; van Wijngaarden, J. Fourier Transform Microwave Spectra of a New Isomer of OCS-CO_2. *J. Chem. Phys.* **2009**, *131* (4), 044303.

(16) Pracht, P.; Bohle, F.; Grimme, S. Automated Exploration of the Low-Energy Chemical Space with Fast Quantum Chemical Methods. *Phys. Chem. Chem. Phys.* **2020**, *22* (14), 7169–7192.

(17) Bannwarth, C.; Ehlert, S.; Grimme, S. GFN2-XTB - An Accurate and Broadly Parametrized Self-Consistent Tight-Binding Quantum Chemical Method with Multipole Electrostatics and Density-Dependent Dispersion Contributions. *J. Chem. Theory Comput.* **2019**, *15* (3), 1652–1671.

(18) Grimme, S. Semiempirical Hybrid Density Functional with Perturbative Second-Order Correlation. *J. Chem. Phys.* **2006**, *124* (3), 034108.

(19) Grimme, S.; Ehrlich, S.; Goerigk, L. Effect of the Damping Function in Dispersion Corrected Density Functional Theory. *J. Comput. Chem.* **2011**, *32* (7), 1456–1465.

(20) Grimme, S.; Antony, J.; Ehrlich, S.; Krieg, H. A Consistent and Accurate Ab Initio Parametrization of Density Functional Dispersion Correction (DFT-D) for the 94 Elements H-Pu. *J. Chem. Phys.* **2010**, *132* (15), 154104.

(21) Weigend, F.; Ahlrichs, R. Balanced Basis Sets of Split Valence, Triple Zeta Valence and Quadruple Zeta Valence Quality for H to Rn: Design and Assessment of Accuracy. *Phys. Chem. Chem. Phys.* **2005**, *7* (18), 3297–3305.

(22) Boys, S. F.; Bernardi, F. The Calculation of Small Molecular Interactions by the Differences of Separate Total Energies. Some Procedures with Reduced Errors. *Mol. Phys.* **1970**, *19* (4), 553–566.

(23) Frisch, M. J.; Trucks, G. W.; Schlegel, H. B.; Scuseria, G. E.; Robb, M. A.; Cheeseman, J. R.; Scalmani, G.; Barone, V.; Petersson, G. A.; Nakatsuji, H., et al. *Gaussian 16*, Revision C.01; Gaussian, Inc.: Wallingford, CT, 2016.

(24) Keith, T. A. *AIMALL*, version 17.11.14; TK Gristmill Software: Overland Park, KS, 2016.

(25) Contreras-García, J.; Johnson, E. R.; Keinan, S.; Chaudret, R.; Piquemal, J.-P.; Beratan, D. N.; Yang, W. NCIPLOT: A Program for Plotting Noncovalent Interaction Regions. *J. Chem. Theory Comput.* **2011**, *7* (3), 625–632.

(26) Hohenstein, E. G.; Sherrill, C. D. Density Fitting of Intramonomer Correlation Effects in Symmetry-Adapted Perturbation Theory. *J. Chem. Phys.* **2010**, *133* (1), 014101.

(27) Parrish, R. M.; Burns, L. A.; Smith, D. G. A.; Simmonett, A. C.; DePrince, A. E.;

Hohenstein, E. G.; Bozkaya, U.; Sokolov, A. Y.; Di Remigio, R.; Richard, R. M.; et al. Psi4 1.1: An Open-Source Electronic Structure Program Emphasizing Automation, Advanced Libraries, and Interoperability. *J. Chem. Theory Comput.* **2017**, *13* (7), 3185–3197.

(28) Juanes, M.; Lesarri, A.; Pinacho, R.; Charro, E.; Rubio, J. E.; Enríquez, L.; Jaraíz, M. Sulfur Hydrogen Bonding in Isolated Monohydrates: Furfuryl Mercaptan versus Furfuryl Alcohol. *Chem. - A Eur. J.* **2018**, *24* (25), 6564–6571.

(29) Kisiel, Z. PROSPE - Programs for ROtational SPEctroscopy http://www.ifpan.edu.pl/~kisiel/prospe.htm (accessed Jan 15, 2021).

(30) Watson, J. K. G. *In Vibrational Spectra and Structure: A Series of Advances*; Durig, J. R., Ed.; Elsevier: New York, 1977, Vol. 6, pp. 1–89.

(31) Huang, W.; Thomas, J.; Jäger, W.; Xu, Y. Tunnelling and Barrier-Less Motions in the 2-Fluoroethanol–Water Complex: A Rotational Spectroscopic and Ab Initio Study. *Phys. Chem. Chem. Phys.* **2017**, *19* (19), 12221–12228.

(32) Kraitchman, J. Determination of Molecular Structure from Microwave Spectroscopic Data. *Am. J. Phys.* **1953**, *21* (1), 17–24.

(33) van Wijngaarden, J.; Van Nest, S. J.; van Dijk, C. W.; Tokaryk, D. W. Rovibrational Spectrum and Analysis of the N8 Band of Thiophene Using Infrared Synchrotron Radiation. *J. Mol. Spectrosc.* **2010**, *259* (1), 56–59.

(34) Legon, A. C.; Ottaviani, P. The Rotational Spectrum of Thiophene···HBr and a Comparison of the Geometries of the Complexes B···HX, Where B Is Benzene, Furan or Thiophene and X Is F, Cl or Br. *Phys. Chem. Chem. Phys.* **2004**, 488–494.

(35) Espinosa, E.; Molins, E.; Lecomte, C. Hydrogen Bond Strengths Revealed by Topological Analyses of Experimentally Observed Electron Densities. *Chem. Phys. Lett.* **1998**, *285* (3–4), 170–173.

TOC Graphic